

## NMR in AgPt alloys

H. Herberg and J. Voitländer

*Institut für Physikalische Chemie der Universität München, D-8000 München 2, West Germany*

(Received 25 March 1980)

Pulsed NMR and susceptibility measurements were performed on dilute silver-rich  $\text{Ag}_c\text{Pt}_{1-c}$  alloys ( $c = 0.9-1.0$ ). The Knight shift,  $T_1$  and  $T_2$  of  $^{109}\text{Ag}$  and  $^{195}\text{Pt}$  could be observed in magnetic fields up to 5.2 T and at temperatures between 4.2 and 60 K. In  $\text{Ag}_{99.5}\text{Pt}_{0.5}$  a SEDOR experiment (spin echo double resonance) was performed. The different temperature dependencies of the  $^{109}\text{Ag}$  and the  $^{195}\text{Pt}$  resonances indicate the existence of  $d$  holes on Pt sites even in silver-rich alloys. A graphical method in terms of free-electron phase shifts gives a value of  $0.33 \pm 0.07$   $d$  holes which is only about 20% less than in pure platinum. This corresponds closely to the results of Sang and Myers in AgPd alloys where a similar small charge transfer is found and which thus contradicts rigid-band considerations. With a model of Dworin and Narath the  $^{195}\text{Pt}$  Knight shift and the  $^{195}\text{Pt}$  relaxation rate  $T_1^{-1}$  could be divided into  $s$ ,  $d$ , and orbital contributions. Whereas  $d$  and orbital terms approximately cancel numerically,  $K$  and  $T_1^{-1}$  are dominated by  $s$  effects. It is shown why this does not contradict the observed temperature dependencies of  $K$ ,  $T_1^{-1}$ , and the magnetic susceptibility  $\chi$ .

### I. INTRODUCTION

Pulsed nuclear magnetic resonance is one of the most powerful methods to derive static and dynamic hyperfine properties. This has led to an increased understanding of local magnetic properties. In binary alloys, however, a great amount of information often cannot be obtained, because only *one* constituent is observable. In most cases quadrupole interactions are responsible which either disturb the NMR signal completely or produce difficulties with second-order shifts which are hard to distinguish from Knight shifts.

One of the very few systems where these problems do not arise is AgPt. Both nuclei ( $^{109}\text{Ag}$  or  $^{107}\text{Ag}$  and  $^{195}\text{Pt}$ ) possess spin  $I = \frac{1}{2}$  and thus no quadrupole moment. The sensitivity for NMR is quite good. Nevertheless there are only very few measurements on this system.<sup>1</sup> Most probably the reason for this is the apparently complicated phase diagram which shows very restricted solid solubility.<sup>1</sup> But as the diffusion constants in the system AgPt are extremely slow the equilibrium phase boundaries are very difficult to determine. Klement and Luo were able to show that fast quenching techniques from the melt ("splat cooling") yielded single-phase specimens for all compositions.<sup>2</sup> This casts some doubt on the validity of the published phase diagrams. In our investigation we used single-phase specimens up to 10 at. % of Pt in Ag. Neither in x-ray spectra nor in the NMR or susceptibility data could any precipitated second phase be detected.

The alloy system AgPt should be very similar to

the well-known system AgPd: a typical transition metal with a large number of  $d$  holes alloyed with the noble-metal silver. Whereas AgPd suffers from the fact that only silver may be observed by NMR (palladium has a small gyromagnetic ratio  $\gamma$  and a large quadrupole moment) in AgPt *both nuclei* are detectable. This should give far more information about electronic properties as has been shown in a couple of other alloy systems.<sup>3,4</sup>

Recent measurements of Dingle temperatures on dilute silver-rich AgPd alloys and their interpretation in terms of a phase-shift analysis showed that about 0.27  $d$  holes remained on Pd sites even at extremely low Pd concentrations.<sup>5</sup> This agrees qualitatively with coherent-potential-approximation (CPA) calculations and photoemission measurements (where the virtual bound state of Pd in Ag may be easily observed), but is in disagreement with all rigid band considerations.<sup>6</sup> Difficult to understand is the composition and temperature dependence of the magnetic susceptibility, where no indication of  $d$  holes can be found.<sup>7</sup> It seems interesting to compare this situation with that of AgPt.

### II. EXPERIMENTAL

All measurements were performed with a Bruker pulsed NMR spectrometer SXP 4-100, delivering  $H_1$  fields up to 5 mT. For more complicated pulse sequences, such as saturation combs for  $T_1$  experiments, we used a home-built pulse generator with a quartz time base. The relatively weak sensitivity of the  $^{109}\text{Ag}$  nucleus calls for low temperatures together

with high magnetic fields. So we used a superconducting magnet (Oxford Instruments) with a maximum field of 5.2 T and a homogeneity of  $10^{-6}$  in a volume of  $1 \text{ cm}^3$  ( $5 \times 10^{-6}$  in  $8 \text{ cm}^3$ ). The linewidth of  $\text{D}_2\text{O}$  at 300 K was 4.5 Hz and the homogeneity is thus fully sufficient for the broad lines on metallic systems. The large 49-mm bore of the magnet greatly facilitated the construction of probe heads and reduced magneto-acoustic ringing effects. The temperature of the probe could be varied between 1.2 and 300 K. When the magnet was run in the persistent mode, the field was calibrated against the NMR signal of pure silver metal, where the gyromagnetic ratio of  $^{109}\text{Ag}$  is known rather precisely<sup>8</sup> to be  $\gamma_{\text{Ag}} = 0.199\,150(4) \text{ MHz/T}$ . If the magnet is driven by its power supply a voltage of 0–70 mV (proportional to the current) can be measured with a digital voltmeter and calibrated against the  $^{109}\text{Ag}$  signal. No significant stability problems with the power supply or the voltmeter were found; nevertheless, this is the main error in measuring Knight shifts.

For the probe head we used a series  $LC$  circuit with a  $\frac{1}{4} \lambda$  arrangement. The essential details were a semirigid coaxial cable and a variable capacitor (tunable at helium temperatures and nearly temperature independent) mounted very close to the coil. The signal-to-noise ratio was about twice as good as with a simpler probe head, where the capacitor was kept at room temperature and connected to the coil through a long cable (e.g.,  $\frac{1}{2} \lambda$ ). The large bore of the magnet made it possible to use a solenoid instead of Helmholtz coils which results in greater sensitivity.

As the spin echoes were very narrow (10–100  $\mu\text{sec}$ ) we used a transient recorder (Canberry DL 905, 5 MHz) as a fast digitizer. The data were then transferred via an interface to a PDP 11/10 computer and displayed on a large screen. The data transfer was done by an assembler subroutine. This had been added to the so-called SPARTA program (signal processing and real-time analysis, program written by Digital Equipment) which performs all necessary data manipulations such as normalization, subtraction of background spectra, display, output to plotter, Fourier transformation, etc. When the NMR signal was strong enough so that no averaging was necessary, we used a boxcar integrator to measure the spin-echo profiles. The large time constant of the superconducting magnet makes it more difficult to measure the magnetic field exactly.

A sensitivity test of the whole arrangement was performed by the first NMR measurement of metallic zinc, which had long been searched for by various workers.<sup>9</sup>

For SEDOR (spin echo double resonance) we used a Matec spectrometer together with the Bruker SXP4-100. The SEDOR coil had an inner solenoid (for the Pt-NMR) and an outer (orthogonal) pair of Helmholtz coils for the Ag NMR.

For susceptibility measurements we used a Faraday balance which could detect a change of susceptibility  $\chi$  of  $2 \times 10^{-9} \text{ cm}^3/\text{g}$  with an accuracy of 1%. To eliminate the influence of ferromagnetic impurities, the field dependence of  $\chi$  was measured and Honda-Owen extrapolations performed. Usually the samples were only very slightly contaminated.

Besides in pure silver and pure platinum a free induction decay could only be measured in  $\text{Ag}_{99.5}\text{Pt}_{0.5}$ . With increasing impurity content the inhomogeneous distribution of Knight shifts made it necessary to use spin-echo techniques. Spin-lattice relaxation times  $T_1$  were measured by usual  $180^\circ\text{-}\tau\text{-}90^\circ$  sequence or more often by saturation combs ( $n\,90^\circ\text{-}90^\circ\text{-}\tau\text{-}180^\circ$ ). The great number of pulses sometimes caused problems with pulse heating effects.  $T_2$  values or Ruderman-Kittel constants in Pt-rich AgPt alloys were derived from  $90^\circ\text{-}\tau\text{-}180^\circ$  sequences. As the spin echoes were very narrow the Knight shift  $K$  had to be derived from spin-echo profiles (which are plots of echo intensity versus magnetic field). Here the problem arises that in order to get correct results, rather long pulses (equivalent to small  $H_1$  fields) have to be used, which means a small number of excited nuclei and accordingly a reduced signal-to-noise ratio.

We also performed SEDOR experiments in  $\text{Ag}_{99.5}\text{Pt}_{0.5}$  and  $\text{Ag}_{99}\text{Pt}_1$ . The Pt spin-echo intensity  $J(\text{Pt})$  is recorded by a  $90^\circ\text{-}\tau\text{-}180^\circ$  sequence, while simultaneously with the  $180^\circ$  pulse the silver nuclei are irradiated with a variable frequency  $\nu$  (Ag). If one uses the Larmor frequency of the silver nuclei which are neighbors to the Pt nucleus and which thus produce the local field for the Pt echo, a strong decrease of  $J(\text{Pt})$  is found.<sup>10</sup> So the SEDOR technique gives valuable information about the neighborhood of the Pt nucleus.

### III. THEORETICAL CONSIDERATIONS

All considerations from now on are restricted to dilute nonmagnetic substitutional binary alloys, where the host is a simple metal. The model of a free-electron gas is applied to the case of noble metals, especially for silver. This seems justified because experiments have shown nearly spherical Fermi surfaces and rather low-lying  $d$  bands ( $\approx 2 \text{ eV}$  below the Fermi level  $E_F$  for Ag,  $\approx 1 \text{ eV}$  for Cu, Au<sup>11</sup>). Apart from this it has recently been shown that the application of the free-electron gas model is reasonable for the following considerations.<sup>12</sup> When an impurity (platinum) is added to the noble metal (silver), the conduction electrons which are treated as plane waves are scattered at the impurity potential. The solution of this problem gives a set of phase shifts for the partial waves, equivalent to a new arrangement of charge in the vicinity of the impurity atom.<sup>13</sup>

The requirement of charge neutrality is fulfilled via the Friedel sum rule

$$Z_{\text{eff}} = \frac{2}{\pi} \sum_l (2l+1) \delta_l(E_F) , \quad (1)$$

where  $\delta_l(E_F)$  are the phase shifts at the Fermi level and  $Z_{\text{eff}}$  is the extra charge introduced by the impurity (modified according to a formula by Blatt which accounts for variation in the lattice parameter<sup>14</sup>).  $Z_{\text{eff}}$  may be divided into  $s$ ,  $p$ , and  $d$  contributions

$$Z_s = \frac{2}{\pi} \delta_0, \quad Z_p = \frac{6}{\pi} \delta_1, \quad Z_d = \frac{10}{\pi} \delta_2 ; \quad (2)$$

$Z_d$  corresponds to the number of  $d$  holes which will later be designated as  $q$ . The charge screening mainly takes place within the Wigner-Seitz cell but also leads to long-ranged "Friedel oscillations."

This means that the neighbors of the impurity in the next few shells experience different local fields and thus give rise to different lines in the NMR spectrum. Normally this satellite structure cannot be resolved and gives only a concentration-dependent line broadening. Modern techniques were able to resolve up to eight satellites for magnetic impurities.<sup>15</sup> The relative Knight shift of the neighbor shells is given by

$$\begin{aligned} \Gamma(R) &= \frac{\Delta K}{K} \\ &= \sum_l (2l+1) \{ [\eta_l(kR) - j_l(kR)] \sin^2 \delta_l(E_F) \\ &\quad - j_l(kR) \eta_l(kR) \sin[2\delta_l(E_F)] \} , \end{aligned} \quad (3)$$

where  $\eta_l$  and  $j_l$  are Neumann and Bessel functions and  $R$  is the radius of this shell.<sup>16</sup>  $\Gamma(R)$  may be measured by satellite observation or SEDOR techniques.

The mean Knight shift also changes with impurity content and can be quantitatively related to the phase shifts  $\delta_l(E_F)$

$$\Gamma = \frac{1}{c} \frac{\Delta K}{K} = \sum_l \{ \alpha_l \sin^2 \delta_l(E_F) + \beta_l \sin[2\delta_l(E_F)] \} , \quad (4)$$

where  $\alpha_l$  and  $\beta_l$  are constants.<sup>16</sup>

If the energies involved ( $E \leq E_F$ ) are small in comparison to the depth of the scattering potential, only the lowest-order phase shifts (usually  $\delta_0$ ,  $\delta_1$ ,  $\delta_2$ ) have to be regarded.<sup>17</sup>

There are some attempts to calculate the phase shifts from first principles which were quite successful in the case of nontransitional impurities (like Mg in Al, Ge in Cu, Sn in Li) but failed for transitional impurities (like Cr in Al).<sup>18</sup> In any case the impurity potential has to be calculated self-consistently. Daniel tried to calculate Knight shifts with a square-

well potential whose depth was adjusted by means of the Friedel sum rule.<sup>16</sup> This procedure, however, gives bad results for transitional impurities (e.g., the wrong sign for AgPt alloys) where resonance scattering effects become important and perhaps dominate potential scattering. This means that either very refined calculations are necessary or *semiempirical phase shifts* have to be used. These may be derived from Dingle-temperature measurements, from optical reflectivity, wipe-out numbers, residual electrical resistivity, Knight shift, or any other physical quantity that can quantitatively be related to phase shifts. A well-known example is the relation between the residual electrical resistivity  $\Delta_p$  and the phase shifts  $\delta_l(E_F)$  which is given by<sup>19</sup>

$$\Delta_p = \frac{4\pi c}{Z_0 k_F} \sum_l l \sin^2 [\delta_l(E_F) - \delta_{l+1}(E_F)] . \quad (5)$$

#### IV. MEASUREMENTS AND DISCUSSION

##### A. $d$ holes on platinum

Figure 1 shows a spin echo of the  $^{109}\text{Ag}$  resonance in  $\text{Ag}_{99}\text{Pt}_1$  (later the following convention is used: *Italic Ag* or *Pt* means that this is the nucleus under inspection).

Among the very few NMR experiments on AgPt alloys, Snodgrass measured temperature variations of linewidth and Knight shift in very dilute silver-rich alloys.<sup>20</sup> He found a nearly constant Knight shift, but a marked variation of the linewidth. This led him to the assumption that  $d$  holes on Pt sites should exist.

In our pulse measurements we used higher Pt concentrations (from 0.5 to 10 at. %) and detected more pronounced effects. The spin-spin-relaxation time  $T_2$  was considerably temperature dependent at high Pt concentrations (a decrease of about 25% from 4.2 to 60 K). This is far more than can be explained by the influence of spin-lattice relaxation. Towards the very dilute alloys, the temperature dependence of  $T_2$  becomes smaller and can no longer be precisely measured within the error bars. Measurements at much higher temperatures would be useful. The behavior

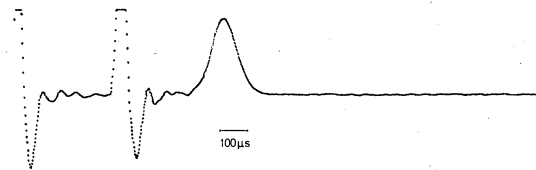


FIG. 1.  $90^\circ\text{-}\tau\text{-}180^\circ$  spin echo in  $\text{Ag}_{99}\text{Pt}_1$  ( $^{109}\text{Ag}$  resonance): 4 scans at  $T = 4.2$  K, 2  $\mu\text{sec}$  per point, 1024 points.

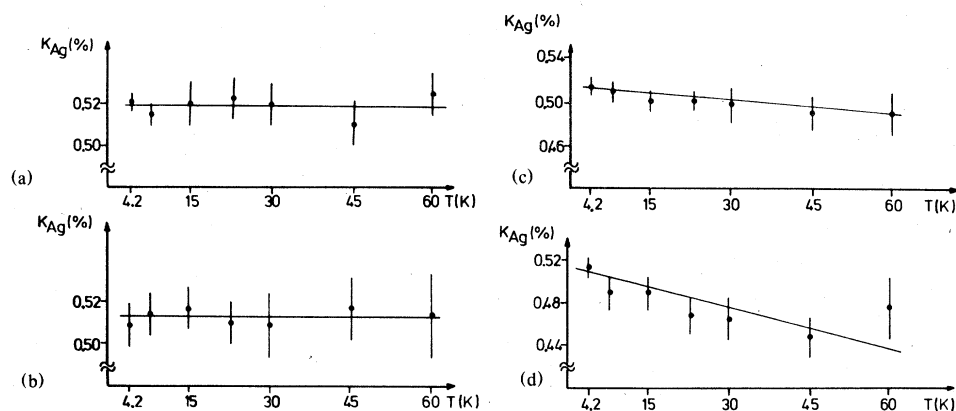


FIG. 2. Temperature dependence of the  $^{109}\text{Ag}$  Knight shift in (a)  $\text{Ag}_{99.5}\text{Pt}_{0.5}$ , (b)  $\text{Ag}_{99}\text{Pt}_1$ , (c)  $\text{Ag}_{95}\text{Pt}_5$ , and (d)  $\text{Ag}_{90}\text{Pt}_{10}$ . All points result from spin-echo profiles.

of  $T_2$  corresponds to Snodgrass's results concerning the linewidth in cw experiments. The  $^{109}\text{Ag}$  Knight shift also shows a temperature dependence which increases with Pt concentration [(Figs. 2a–2d)]. In Figs. 2(a) and 2(b) (the concentration range investigated by Snodgrass) no effect can be seen due to the large error bars, whereas Figs. 2(c) and 2(d) show a concentration-dependent decrease of the Knight shift. This may be attributed to the increased number of silver atoms which are nearest neighbors to a platinum atom and feel a temperature-dependent perturbation caused by the Pt atom. As the effect in  $\text{Ag}_{95}\text{Pt}_5$  and in  $\text{Ag}_{90}\text{Pt}_{10}$  is different, a loosely defined "perturbation radius  $\lambda$ " of about one lattice constant may be derived. This means a rather good charge screening of the Pt impurities and confirms that even  $\text{Ag}_{90}\text{Pt}_{10}$  may be regarded as "dilute." (The definition "dilute" depends on screening considerations and far less on absolute concentrations.)

The values of the Knight shift, extrapolated to  $T = 0$  K, as a function of impurity concentrations give

$$\Gamma = \frac{1}{c} \frac{\Delta K}{K} = -0.2 \pm 0.2 .$$

This value does not contradict the measurements of Snodgrass in AgPt ( $\Gamma \approx 0$ ) and happens to have the same value as in AgPd alloys.<sup>1</sup>

The measurements of the  $^{195}\text{Pt}$  Knight shift and relaxation rates in dilute AgPt alloys was more difficult because of limited signal-to-noise ratios. Apart from rather constant  $T_1 T$  values we found an extremely strong temperature dependence of  $T_2$  which cannot be attributed to spin-lattice relaxation effects alone (Fig. 3). The platinum Knight shift also showed a strong temperature variation (about 1% change per 10 K) which does not change with platinum concentration [Figs. 4(a)–(d)].

All these observations are consistent if, in agreement with Snodgrass, *d holes on Pt sites* are assumed which produce the temperature effects. The number of *d holes* seems to be rather constant up to 10 at. % Pt which is reflected in the same temperature dependence for all four alloys (Fig. 4). This corresponds, at least in part, to the short screening radius  $\lambda$  of about one lattice constant.

This model of *d holes* on Pt sites even in very silver-rich AgPt alloys clearly contradicts any rigid-band considerations which postulate a filled, common (and rigid) *d band* for alloys with more than about 60 at. % Ag.

There are a couple of experiments and calculations that further support this view (not for AgPt, but for similar virtual-bound-state alloys): (a) Sang and Myers recently measured anisotropies of Dingle temperatures in very dilute silver-rich AgPd single crystals and derived a number of 0.27 *d holes*.<sup>5</sup> This fig-

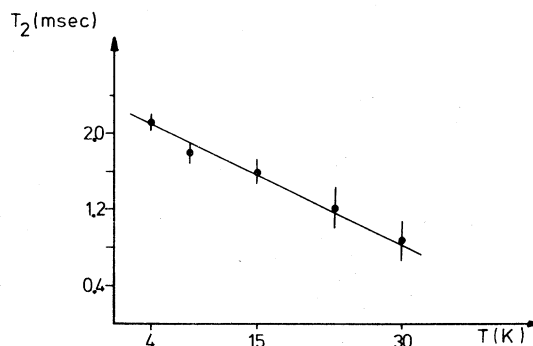


FIG. 3.  $T_2$  of  $^{195}\text{Pt}$  in  $\text{Ag}_{95}\text{Pt}_5$  measured by a  $90^\circ\text{-}\tau\text{-}180^\circ$  sequence.

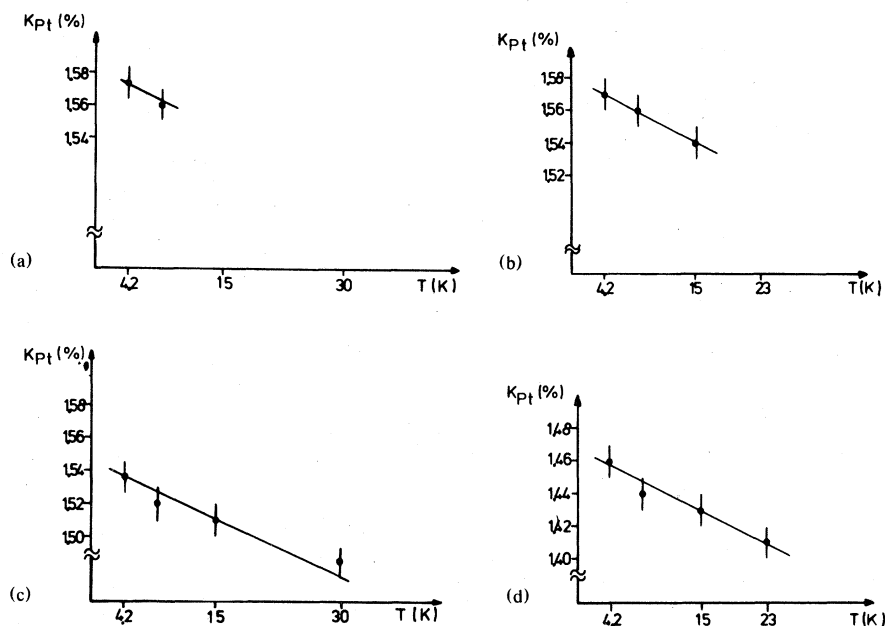


FIG. 4. Temperature dependence of the  $^{195}\text{Pt}$  Knight shift in (a)  $\text{Ag}_{99.5}\text{Pt}_{0.5}$ , (b)  $\text{Ag}_{99}\text{Pt}_1$ , (c)  $\text{Ag}_{95}\text{Pt}_5$ , and (d)  $\text{Ag}_{90}\text{Pt}_{10}$ . All points result from spin-echo profiles.

ure has to be compared to 0.36  $d$  holes in pure palladium metal.<sup>21</sup> (b) Ertl and Wandelt detected  $d$  holes in copper-rich CuNi alloys by appearance-potential spectroscopy (APS).<sup>22</sup> (c) Béal-Monod calculated semiempirical phase shifts for the systems CuPt, CuRh, and CuNi from wipe-out numbers, residual electrical resistivity, and the Friedel sum rule. This leads to a  $5d^9$  configuration and not to a filled  $d$  shell.<sup>23</sup> (d) CPA calculations for silver-rich AgPd alloys seem to indicate 0.1–0.2  $d$  holes on Pt sites.<sup>6</sup>

As accurate *ab initio* calculations are not yet available we now try to derive the number of  $d$  holes in AgPt alloys by a semiempirical phase-shift analysis. For this purpose we adopt the Eqs. (1), (4), and (5) for the unknown phase shifts  $\delta_0$ ,  $\delta_1$ ,  $\delta_2$  in terms of  $Z_{\text{eff}}$  and the measured quantities  $\Delta\rho$  and  $\Gamma$ . The effective charge  $Z_{\text{eff}}$  is determined from the Blatt correction formula<sup>14</sup> and gives  $Z_{\text{eff}} = -0.85$ . The value of silver was measured to be  $\Gamma = -0.2 \pm 0.2$ .  $\Gamma$  and  $Z_{\text{eff}}$  for AgPt happen to have the same value as for AgPd. The published value of  $\Delta\rho$  in AgPt is  $1.59 \mu\Omega \text{ cm}$  and in AgPd  $0.44 \mu\Omega \text{ cm}$ .<sup>24</sup> Recent investigations of Barber and Caplin in the low-temperature region on extremely dilute alloys showed considerable difficulties in measuring  $\Delta\rho$ .<sup>25</sup> Nevertheless an approximate value of  $\Delta\rho(\text{AgPt}) = 1.32 \mu\Omega \text{ cm}$  may be derived from these experiments. It remains to be shown how these discrepancies influence the following analysis. As it is necessary to see how small variations in all parameters of Eqs. (1), (4), and (5)

change the solutions, it seems appropriate to use a graphical method to solve Eqs. (1), (4), and (5).

First,  $\delta_0$  is eliminated to get two transcendental equations with two unknowns  $\delta_1$  and  $\delta_2$ . Figures 5 and 6 show the contour line diagrams of these equations for different values of  $\Delta\rho$  and  $\Gamma$ . As these diagrams are periodic in  $\pi$ , only the range  $-\frac{1}{2}\pi \leq \delta_1$ ,  $\delta_2 \leq \frac{1}{2}\pi$  is shown.

As the temperature dependencies of  $K$  and  $T_2$  for the  $^{109}\text{Ag}$  and the  $^{195}\text{Pt}$  NMR had indicated the ex-

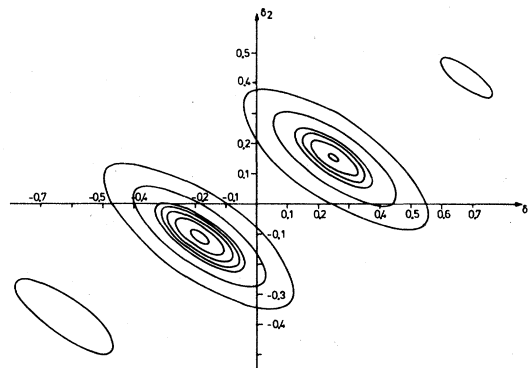


FIG. 5. Contour line diagrams for  $\Delta\rho$  as a function of the phase shifts  $\delta_1$  and  $\delta_2$ . The  $\Delta\rho$  values were 0.24, 0.4, 0.56, 0.72, 0.88, 1.6,  $3.0 \Omega \text{ cm}$ , beginning from the inner ellipses.

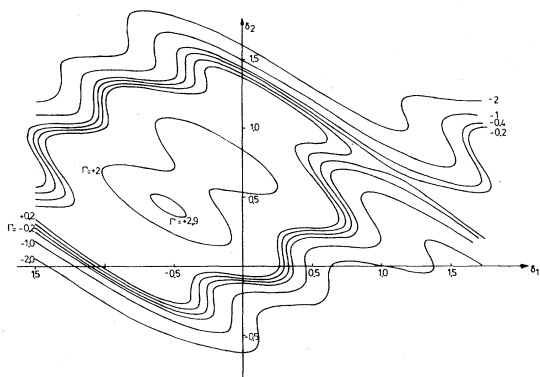


FIG. 6. Contour line diagrams for  $\Gamma$  as a function of  $\delta_1$  and  $\delta_2$  starting from the innermost curve, the parameters are  $\Gamma = +2.9, +2, +0.2, 0, -0.2, -0.4, -1.0, -2.0$ .

istence of  $d$  holes,  $\delta_2$  must be negative. Figure 7 shows that region of the  $\delta_1\delta_2$  plane where  $\delta_2 < 0$  and the contour line diagrams for the appropriate  $\Gamma$  and  $\Delta\rho$  values cross one another. The three  $\Gamma$  curves belong to the experimental value with its error bars:  $\Gamma = -0.2 \pm 0.2$  and are thus valid for AgPt as well as for AgPd. The two  $\Delta\rho$  ellipses (for AgPt and AgPd, respectively) are drawn without error bars, as none are quoted in the work of Barber and Caplin.<sup>25</sup> Figures 5 and 7 show, however, that small changes in  $\Delta\rho$  up to 10 or 20% do not influence the value of  $\delta_2$ . So the range of possible solutions for AgPt is somewhere between  $A$  and  $C$  or between  $D$  and  $F$ . It should be mentioned that this already means a restricted range of  $\delta_2$  values

$$-0.08 \leq \delta_2 \leq -0.2 .$$

Points  $x$  and  $y$  and the inner ellipse refer to the case

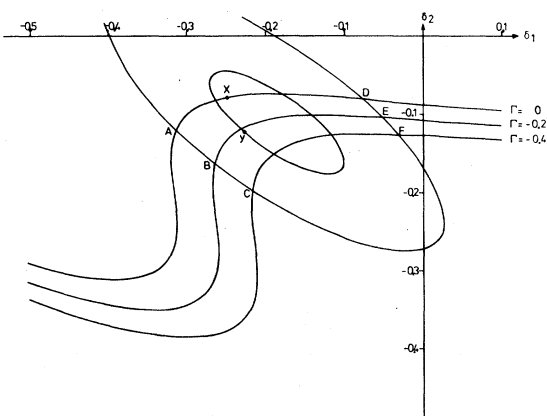


FIG. 7. Crossing of the  $\Delta\rho$  and  $\Gamma$  contour lines: three  $\Gamma$  curves for the experimental value  $-0.2 \pm 0.2$  with its error bars. The outer ellipse belongs to  $\Delta\rho(\text{AgPt})$ , the other to  $\Delta\rho(\text{AgPd})$ .

of AgPd.  $y$  is a solution derived by Béal-Monod by semiempirical methods,<sup>23</sup>  $x$  has been derived by Sang and Meyers from Dingle-temperature anisotropies. It is quite encouraging that for AgPd both points  $x$  and  $y$  lie within the error range of the graphical solution of Eqs. (1), (4), and (5).

There are three arguments which support the view that for AgPt alloys the correct solution has to be found between  $D$  and  $F$  and not between  $A$  and  $C$ : (a) The range  $A-C$  would mean a larger number of  $d$  holes on Pt sites than in pure platinum which seems rather unlikely. (b) Béal-Monod derived semiempirical phase shifts  $\delta_l$  in CuPd and CuPt.<sup>23</sup> This analysis gave more negative  $\delta_0$  and  $\delta_2$  values and a less negative  $\delta_1$  value in CuPt compared to CuPd. If these trends are attributed to the different impurity potential, independent of the host, and thus applicable to the case of AgPd and AgPt, the range  $D-F$  results as the correct solution. (c) We performed a SEDOR experiment in  $\text{Ag}_{99.5}\text{Pt}_{0.5}$  where the result is shown in Fig. 8.

The long vertical bar, designated as  $\nu_0$ , gives the bulk NMR frequency of the Ag nuclei, as detected in a separate experiment in the same probe head.  $\nu_0$  could be measured with an accuracy of  $\pm 200$  Hz which means a negligible error in Fig. 8. The minimum of the SEDOR line  $\bar{\nu}$  cannot be determined precisely, but differs from  $\nu_0$ . The relative change of Knight shift is

$$\Gamma_S = \frac{\Delta K}{K} = (-4.3 \pm 1.3)\% .$$

If the value is tentatively attributed to second-nearest neighbors and the range of  $\delta_0$ ,  $\delta_1$ , and  $\delta_2$  as taken from Fig. 7 is inserted in Eq. (2), no solution can be found. If  $\Gamma_S$  is attributed to nearest neighbors, a contour line in this  $\delta_l$  range may be drawn (dashed lines in Fig. 9). No coincidence of the  $\Gamma_S$  contour lines to

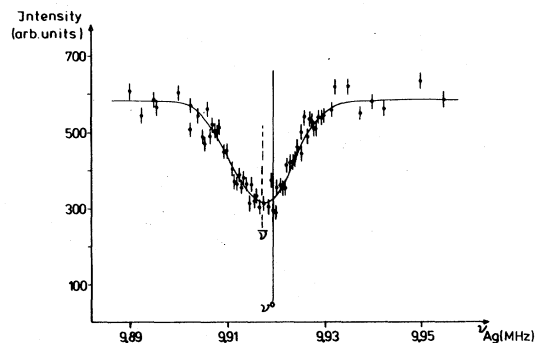


FIG. 8. SEDOR spectrum: the intensity of the  $^{195}\text{Pt}$  echo as a function of  $^{109}\text{Ag}$  frequency. Each data point is an average of 1000 scans.

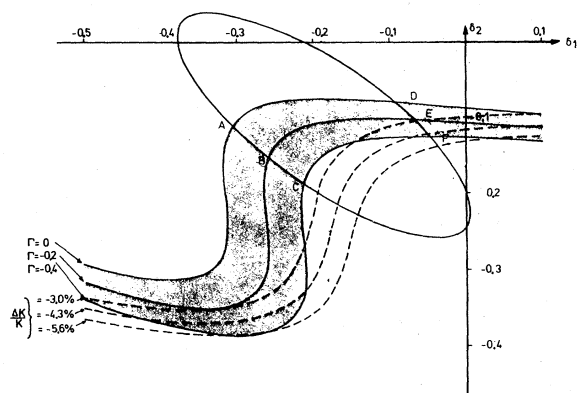


FIG. 9. Crossing of the  $\Delta\rho$ ,  $\Gamma$ , and  $\Gamma_s$  contour line diagrams. The shaded area shows  $\Gamma$  with its error bars, the dashed lines belong to  $\Gamma_s = -4.3 \pm 1.3\%$ .

$A-C$  occurs, but a good agreement within the range  $D-F$ . So we conclude that the solution of Eqs. (1), (4), and (5) lies near point  $E$  which corresponds to the following phase shifts

$$\begin{aligned} -0.7 \leq \delta_0 \leq -0.6, \quad -0.07 \leq \delta_1 \leq -0.03, \\ -0.12 \leq \delta_2 \leq -0.08. \end{aligned}$$

According to Eq. (2) the number of  $d$  holes is given by<sup>16</sup>

$$q = 0.33 \pm 0.07.$$

This means that the number of  $d$  holes on Pt sites in dilute AgPt alloys has not changed very much as compared to pure platinum ( $q \approx 0.43$ ). The decrease of  $q$  of about 20% is comparable to the case of AgPd. A nonzero value of  $q$  in silver-rich alloys shows a breakdown of rigid-band considerations (also for the modified version of Dugdale and Guenault).<sup>26</sup> The minimum polarity model of Lang and Ehrenreich would predict the same number of  $d$  holes per Pt atom as in pure platinum.<sup>27</sup> So the reality is somewhere between these two extremes and quite obviously far more similar to the "neutral-atom" configuration of the minimum polarity model. The charge transfer from Ag to Pt seems to be rather small, but nonzero. This conclusion compares favorably to the results of Kleiman *et al.*<sup>28</sup> in CuPt alloys.

### B. Origin of $K(\text{Pt})$ and $T_1(\text{Pt})$

As already shown in Fig. 4, the platinum Knight shift in silver-rich alloys is rather large and positive ( $K = +1.58\%$  for  $c \rightarrow 0$ ,  $T \rightarrow 0$ ). The relaxation rate  $T_1^{-1}$  has about twice the value of pure Pt. To get some feeling for the origin of these values, one can break down  $K$  and  $T_1$  into  $s$ ,  $d$ , and orbital contribu-

tions<sup>29</sup>

$$K_{\text{expt}} = K_s + K_d + K_{\text{orb}}, \quad (6)$$

$$T_{1\text{expt}}^{-1} = T_{1s}^{-1} + T_{1d}^{-1} + T_{1\text{orb}}^{-1}, \quad (7)$$

where  $K_{\text{expt}}$  and  $T_{1\text{expt}}^{-1}$  stands for the experimental values. As has been done successfully for the case of pure Pt it is assumed that no  $s-d$  mixing occurs.<sup>30,31</sup>

With a slightly modified Anderson operator Dworin and Narath derived two Korringa relations for the  $d$  and orbital parts of  $K$  and  $T_1$  (Ref. 32)

$$K_d^2 T_{1d} T = 5S, \quad (8)$$

$$K_{\text{orb}}^2 T_{1\text{orb}} T = 10S, \quad (9)$$

$$S = \frac{\gamma e \hbar}{\gamma_n 4\pi K_B}. \quad (9)$$

These formulas have often been applied to the case of  $3d$  impurities in simple hosts, where it can be shown that  $s$  effects are negligible.<sup>29</sup> Then the resulting four Eqs. (6)–(9) are easy to solve. For AgPt alloys, however, we cannot neglect  $s$  effects. Thus we introduce a third Korringa relation for the  $s$  parts with an unknown, variable enhancement factor  $\alpha$ :

$$K_s^2 T_{1s} T = \alpha S. \quad (10)$$

$\alpha = 1$  corresponds to free, noninteracting  $s$  electrons and is thus a lower limit for  $\alpha$ . For pure silver a value of  $\alpha = 2.0 \pm 0.2$  has been found which most probably contains not only  $s$  effects.<sup>33</sup> So we regard a value of  $\alpha = 2.2$  as an upper bound for our following estimates. The delocalization of the  $s$  electrons should mean that the enhancement properties of the silver host are responsible for Eq. (10).

To solve Eqs. (6) and (10) (five equations, but seven unknowns) we adopt the following sign conventions which have been extensively discussed in

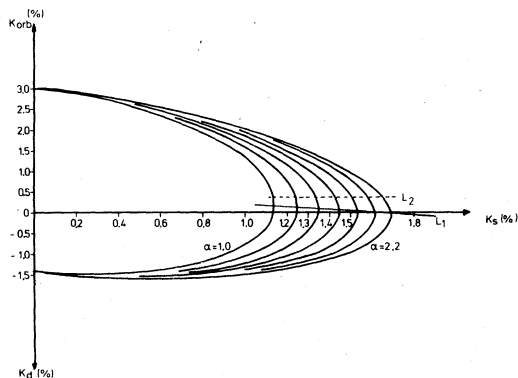


FIG. 10. Graphical solution of Eqs. (6) to (10), see text.

the literature:

$$K_s > 0, K_d < 0, K_{orb} > 0. \quad (11)$$

Figure 10 shows  $K_{orb}$  and  $K_d$  as a function of  $K_s$  with  $\alpha$  as a parameter. All lines below the slightly inclined line  $L_1$  represent  $K_d$  curves, the curves above  $L_1$  represent  $K_{orb}$  curves. The small region between the  $K_s$  axis and  $L_1$  shows solutions which contradict Eq. (11) and are thus discarded. To find some more restrictions we first tried to analyze the different temperature dependencies of  $K(\text{Pt})$  and  $T_1(\text{Pt})$ . However, the experimental error bars in the  $T_1$  measurements were too big to allow any further analysis.

Therefore the following assumptions were made:

(a) The orbital hyperfine field on Pt sites has *not* changed compared to pure Pt metal. This assumption is not very restrictive, as the same physical conclusions (with only minor numerical changes) resulted if a slightly different hyperfine field was assumed. (b) The  $d$  hyperfine field has the same value as in Pt metal. (c) A formula for the local orbital susceptibility (postulated by Clogston *et al.*<sup>30</sup>) may be applied

$$K_{orb} \sim \chi_{orb} \sim q(10-q). \quad (12)$$

Assumption (a) seems to be supported by photoemission measurements in AgPt which showed a spin-orbit coupling constant  $\xi$  (closely related to  $H_{orb}$ ) of about the same size as in pure Pt metal.<sup>34</sup> Assumption (c) leads to a "scaling" of  $K_{orb}$  in AgPt relative to pure Pt:

$$K_{orb}(\text{AgPt}) = \frac{q_1(10-q_1)}{q_2(10-q_2)} K_{orb}(\text{Pt}),$$

$$q_1 = q(\text{AgPt}) = 0.33, \quad q_2 = q(\text{Pt}) = 0.43.$$

The resulting value of  $K_{orb}(\text{AgPt}) = +0.30\%$  inserted in Fig. 10 gives the horizontal dashed line  $L_2$ . For each  $\alpha$  value the corresponding  $K_d$  may now be extracted.

As the  $d$  and orbital hyperfine field in Pt metal are known from Jaccarino plots,<sup>30,31</sup> the local susceptibilities  $\chi_d$  and  $\chi_{orb}$  can be calculated. The model of Dworin and Narath gives two relations for  $\chi_d$  and  $\chi_{orb}$  in terms of the Anderson parameters  $U$  and  $J$  and the  $d$ -electron density of states  $\rho_d(E_F)$  (Ref. 29)

$$\chi_d = \frac{2\mu_B^2 \rho_d(E_F)}{1 - \frac{1}{5}(U+4J)\rho_d(E_F)}, \quad (13)$$

$$\chi_{orb} = \frac{4\mu_B^2 \rho_d(E_F)}{1 - \frac{1}{5}(U-I)\rho_d(E_F)}. \quad (14)$$

Equations (13) and (14) lead to a useful inequality

$$\chi_{orb} \leq 2\chi_d. \quad (15)$$

Equation (11) together with Eq. (15) restrict the

range of possible solutions in Fig. 10

$$1.5 \leq \alpha \leq 2.2,$$

$$1.4\% \leq K_s \leq 1.66\%,$$

$$-0.44\% \leq K_d \leq -0.21\%,$$

$$22.0 \leq (T_{1s}T)^{-1} \leq 22.6 \text{ sec K}^{-1},$$

$$0.12 \leq (T_{1orb}T)^{-1} \leq 0.17 \text{ sec K}^{-1},$$

$$0.01 \leq (T_{1d}T)^{-1} \leq 0.55 \text{ sec K}^{-1}.$$

We found that the physical meaning of these results was rather independent of the exact value of  $K_{orb}$  (which is equivalent to the number of  $d$  holes). Finally the following conclusions can be drawn: (i) The Knight shift  $K(\text{Pt})$  has a dominating  $s$  contribution  $K_s$ . The nonzero  $d$  and orbital contributions  $K_d$  and  $K_{orb}$  approximately cancel numerically but nevertheless produce the temperature effects. (ii) The relaxation rate is almost completely due to  $s$  effects;  $d$  and orbital terms are very small. (iii) The enhancement factor  $\alpha$  has about the same value as in pure Ag metal.

The smaller value of  $K_d$  compared to pure Pt metal presumably results from a strong decrease in  $d$ -enhancement factors, according to smaller Pt-Pt interactions (because of a short-range screening). The smaller number of  $d$  holes (0.33 instead of 0.43) also indicates a reduced density of states  $\rho_d(E_F)$  which furthermore reduces the small  $K_d$  value. The increased  $K_s$  value as compared to pure Pt metal might be attributed to a larger  $s$ -electron density arising from the Ag matrix. Possibly Korringa-Kohn-Rostoker (KKR) calculations could give detailed information on these points. If the electron density of states  $\rho_d(E_F)$  were known, the  $5d$  Anderson parameters  $U$  and  $J$  could be calculated. To our knowledge no measurements of  $\rho_d(E_F)$  (e.g., via specific electronic heat) for the system AgPt are yet available.

### C. Susceptibility

To check the consistency of the considerations above it seems appropriate to discuss susceptibility measurements of the AgPt system. Unfortunately for our discussion the theoretical work about the relation between  $\chi_d$  and  $\chi_{orb}$  and the bulk susceptibility is not sufficient. Yet in a paper of Klein and Heeger a simple formula is derived under some restricted assumptions<sup>35</sup>

$$\chi_{exp} = \chi_{host} + c\chi_d. \quad (16)$$

Figure 11 shows the concentration dependence of  $\chi_{exp}$ , extrapolated to  $T=0$ ,  $H=\infty$  (Honda-Owen extrapolation).



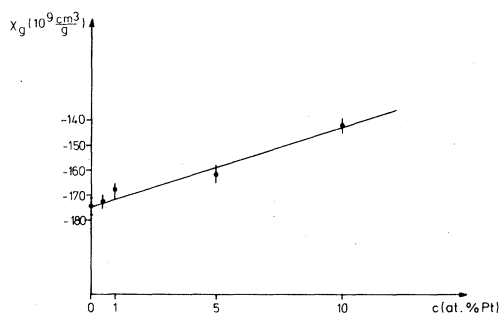


FIG. 11. Magnetic susceptibility  $\chi_g$  in silver-rich AgPt alloys extrapolated to  $T=0$ ,  $H=\infty$  from temperature- and field-dependent measurements.

If we use a somewhat generalized form of Eq. (16)

$$\chi_{\text{exp}} = \chi_{\text{host}} + c(\chi_d + \chi_{\text{orb}}), \quad (17)$$

which seems appropriate as a first approximation, we find  $\chi_d + \chi_{\text{orb}} \approx 0.3 \times 10^{-6} \text{ cm}^3/\text{g}$ . For the case of small enhancement factors the inequality Eq. (15) reduces to  $\chi_d \approx \frac{1}{2} \chi_{\text{orb}}$ . This gives  $\chi_d \approx 0.1 \times 10^{-6}$

$\text{cm}^3/\text{g}$ , and together with the  $d$  hyperfine field of pure platinum  $K_d \approx -0.45\%$ . This value should be compared to  $-0.40 \leq K_d \leq -0.21\%$ . All these figures show that bulk susceptibility experiments are consistent with the given interpretation of the NMR data.

The susceptibility  $\chi_{\text{exp}}$  ought to show a temperature dependence (like the Knight shift does) but no effect could be seen. This is due to the fact that  $\chi$  is a bulk property which in Ag-rich alloys contains only a very small temperature-dependent part (too small to be detectable), whereas NMR measures local properties where  $K_d$  is an appreciable fraction of the measured Knight shift.

#### ACKNOWLEDGMENTS

We would like to thank J. Abart for a great deal of experimental assistance. We are indebted to the Deutsche Gold- und Silberscheideanstalt (DEGUSSA) for the preparation and the loan of the samples. Thanks are also due to the Deutsche Forschungsgemeinschaft for financial support.

- <sup>1</sup>G. C. Carter, L. Bennett, and D. J. Kahan, *Prog. Mater. Sci.* **20**, 1 (1977).
- <sup>2</sup>W. Klement and H. L. Luo, *Trans. Metall. Soc. AIME* **227**, 1253 (1963).
- <sup>3</sup>H. T. Weaver and R. K. Quinn, *Phys. Rev. B* **10**, 1816 (1974).
- <sup>4</sup>H. Alloul, *J. Phys. F* **4**, 1501 (1974).
- <sup>5</sup>D. Sang and A. Myers, *J. Phys. F* **6**, 545 (1976).
- <sup>6</sup>G. M. Stocks, R. W. Williams, and J. S. Faulkner, *J. Phys. F* **3**, 1688 (1973).
- <sup>7</sup>P. Brill and J. Voitländer, *Z. Phys. B* **20**, 369 (1975).
- <sup>8</sup>A. Narath, *Phys. Rev.* **163**, 252 (1967); **175**, 373 (1968).
- <sup>9</sup>H. Herberg, J. Abart, and J. Voitländer, *Z. Naturforsch. Teil A* **34**, 1029 (1979).
- <sup>10</sup>J. B. Boyce, Ph.D. thesis (University of Illinois, Urbana, 1972) (unpublished).
- <sup>11</sup>L. H. Bennett, R. W. Mebs, and R. E. Watson, *Phys. Rev. B* **171**, 611 (1968).
- <sup>12</sup>M. A. Ball and M. S. Farthing, *J. Phys. F* **9**, 1223 (1978).
- <sup>13</sup>A. Blandin and E. Daniel, *J. Phys. Chem. Solids* **10**, 126 (1959).
- <sup>14</sup>F. J. Blatt, *Phys. Rev.* **108**, 285 (1957).
- <sup>15</sup>T. J. Aton and C. P. Slichter, *Phys. Rev. B* **18**, 3377 (1979).
- <sup>16</sup>E. Daniel, Ph.D. thesis (University of Paris, 1959) (unpublished).
- <sup>17</sup>F. Calogero, *Variable Phase Approach to Potential Scattering* (Academic, New York, 1967).
- <sup>18</sup>P. Leonard (private communication).
- <sup>19</sup>G. Grüner, *Adv. Phys.* **23**, 941 (1974).
- <sup>20</sup>R. G. Snodgrass, *Phys. Rev. B* **3**, 3738 (1971).
- <sup>21</sup>J. J. Vuillemin and M. G. Priestley, *Phys. Rev. Lett.* **14**, 307 (1965); J. J. Vuillemin, *Phys. Rev.* **144**, 396 (1966).
- <sup>22</sup>G. Ertl and K. Wandelt, *Phys. Rev. Lett.* **29**, 218 (1972).
- <sup>23</sup>M. T. Béal-Monod, *Phys. Rev.* **164**, 360 (1967).
- <sup>24</sup>J. O. Linde, *Ann. Phys. (Leipzig)* (V) **15**, 219 (1932).
- <sup>25</sup>A. J. Barber and A. D. Caplin, *J. Phys. F* **5**, 679 (1975).
- <sup>26</sup>J. S. Dugdale and A. M. Guenault, *Philos. Mag.* **13**, 503 (1966).
- <sup>27</sup>N. D. Lang and H. Ehrenreich, *Phys. Rev.* **168**, 605 (1968).
- <sup>28</sup>G. G. Kleiman, V. S. Sundaram, C. L. Barreto, and J. D. Rogers, *Solid State Commun.* **32**, 919 (1979).
- <sup>29</sup>A. Narath, *CRC Rev. Solid State Sci.* **2**, 1 (1972).
- <sup>30</sup>A. M. Clogston, V. Jaccarino, and Y. Yafet, *Phys. Rev. A* **134**, 650 (1964).
- <sup>31</sup>M. Shaham, U. El-Hanany, and D. Zamir, *Phys. Rev. B* **17**, 3513 (1978).
- <sup>32</sup>L. Dworin and A. Narath, *Phys. Rev. Lett.* **25**, 1287 (1970).
- <sup>33</sup>G. A. Matzkanin, J. J. Spokas, C. H. Sowers, D. O. van Ostenburg, and H. G. Hovee, *Phys. Rev.* **181**, 559 (1969).
- <sup>34</sup>S. Hüfner, G. K. Wertheim, and J. H. Wernick, *Solid State Commun.* **17**, 585 (1975).
- <sup>35</sup>A. P. Klein and A. J. Heeger, *Phys. Rev.* **144**, 458 (1969).